



Effect of the formulation parameters on the encapsulation efficiency and release behavior of *p*-aminobenzoic acid-loaded ethylcellulose microspheres

MERYEM MOUFFOK¹, ABDERREZZAK MESLI^{1*}, ILHAM ABDELMALEK¹
and ETIENNE GONTIER²

¹Laboratory of Physical and Macromolecular Organic Chemistry, Faculty of Exact Sciences, University of Djillali Liabes, Sidi Bel-Abbes, Algeria and ²Bordeaux Imaging Center–UMS 3420, Victor Segalen, University of Bordeaux, France

(Received 8 March, revised 28 June, accepted 1 July 2016)

Abstract: In the current study, *p*-aminobenzoic acid-loaded ethylcellulose microspheres were prepared under various conditions by the solvent evaporation method (o/w). This preparation was performed with different *p*-aminobenzoic acid:ethylcellulose (PABA:EC) ratios, stirring speeds, surfactant nature and concentrations in order to investigate their effect on the encapsulation efficiency and drug release kinetics. Scanning electron microscopy (SEM) studies showed spherical microspheres with a porous surface and different structures. The mean Sauter diameter (d_{32}) of these microparticles was in the range from 47 to 165 μm with PVA and from 793 to 870 μm with Tween 80 by adjusting process parameters. However, the encapsulation efficiency varied from 37.52 to 79.05 % suitable for the adjustment of a *p*-aminobenzoic acid with prolonged release. The microspheres were characterized by the FTIR, DSC and XRD methods. The release of the cation of *p*-aminobenzoic acid was performed in simulated gastric medium at pH 1.2 and at 37±0.5 °C using UV–Vis analysis to estimate its content. The release data were best fitted to the Higuchi model with high correlation coefficients (r^2) and the values of n obtained from the Korsmeyer–Peppas method showed that the drug release followed the Fickian diffusion mechanism.

Keywords: microparticles; solvent evaporation method; diffusion; drug release; kinetic modeling.

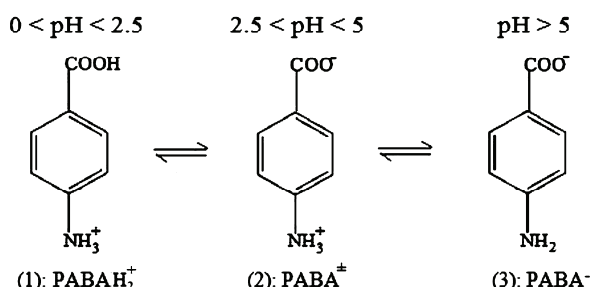
INTRODUCTION

It has long been known that *p*-aminobenzoic acid (PABA) supports the production of tetrahydrofolic acid (THFA), enhances the metabolism of amino acids and improves the formation and health of red blood cells.^{1,2} Among the

* Corresponding author. E-mail: abderrezzak-mesli@netcourrier.com
doi: 10.2298/JSC160308068M

recently determined properties of PABA, its inductor effect on interferon formation in living organisms should be mentioned.³ In addition, it was demonstrated that PABA enhances the treatment efficiency of cornea defaults.⁴ PABA also inhibits melanogenesis *in vitro* and *in vivo*, alone or in combination with chemotherapy (CT). Furthermore, the biological activities of the PABA molecule as an antiviral, antioxidant, antibacterial, antimutagenic and fibrinolytic immunomodulator agent have been demonstrated.⁵ For instance, Akberova established a new antiviral drug Actipol®, which is a 0.007 % PABA solution used in ophthalmology.⁶

Despite of these new biological properties of PABA quoted above, its encapsulation was performed only in the case of a solar filter to protect the skin from UVA/B radiation. Microcapsules of PABA with a hardened polymeric shell can be spread *via* a cream with total elimination of contact between the allergenic PABA and the skin.⁷ PABA is a water-soluble compound constituting the central part of folic acid and thereby considered as a B-complex factor. It is well tolerated with an easy oral administration.⁸ PABA tablet, potassium aminobenzoate capsule, PABA or potassium aminobenzoate are given in food for analytical tests of PABA recovery in 24-h urine collections.⁹ It is required in small amounts by the human body but causes liver damage when used in excess.¹⁰ PABA is an amphoteric compound existing in three forms¹¹ (Scheme 1) in an aqueous environment at physiological pH with two *pK* values (*pK*₁ = 2.50 and *pK*₂ = 4.87). The simulated gastric medium (pH 1.2) promotes the diffusion of the ammonium diacid form (**1**) with a large majority in this study. The simple UV spectrum of **1**, in this case, allows an easy access to PABAH, % released *versus* time. Microencapsulation of PABA in microspheres using ethylcellulose (EC), as a biocompatible polymer matrix, allows its oral administration with sustained release in the stomach at doses below its toxic level. These microparticle dosage forms can be advantageously used for treating skin cancer. The main objective of this study was to elaborate microspheres of *p*-aminobenzoic acid (PABA) for sustained release using microencapsulation by the solvent evaporation method^{12–20} and to study the effects of process parameters, such as stirring



Scheme 1. Forms of *p*-aminobenzoic acid at different pH values.

speed, nature and concentration of the surfactant, and the ratio of PABA:EC on the characteristics of the microspheres, encapsulation efficiency and *in vitro* release behavior. The obtained microspheres were characterized by SEM, FTIR, DSC and XRD. The release from these systems was performed in simulated gastric medium²¹ at pH 1.2 and 37±0.5 °C using UV–Vis analysis to estimate the drug content and the influence of different process parameters is discussed. The obtained release data were analyzed according to the Higuchi and the Korsmeyer–Peppas models to determine the PABA H^+ release mechanism.

EXPERIMENTAL

Materials

PABA (*p*-aminobenzoic acid of 99 % purity, Chemical, China), was chosen as the model drug.

Ethylcellulose (EC, viscosity: 10 cP*, 5 % in toluene/ethanol 80:20, extent of labeling: 48% ethoxyl) was purchased from Sigma–Aldrich. Dichloromethane (DCM, purity >98 %) was from Fluka. Polyethylene glycol sorbitan monooleate (Tween 80) and poly(vinyl alcohol) (PVA, 87–89 % hydrolyzed, M_w 13000–23000 g mol⁻¹) were from Sigma. For kinetic measurements, a simulated acidic test solution²² pH 1.2 was prepared by dissolving 2 g of NaCl and 60 mL of HCl solution (1 M) in 1 L of deionized water.

Preparation of microspheres

PABA-loaded ethylcellulose microspheres were prepared using the oil-in-water solvent evaporation method.^{15,20} The effect of various formulation and processing parameters on the characteristics of the microspheres were investigated by varying PABA:EC ratio, stirring speed and the nature and concentration of the surfactant. Ethylcellulose (EC) was dissolved in 32 g of dichloromethane (different amounts of EC 0.25, 0.5, 0.75 and 1 g were used, for changing the PABA:EC ratio: 1:1, 1:2, 1:3 and 1:4). Then, an amount of PABA was dispersed in this solution and stirred at 30 °C. This organic phase was slowly poured into 100 mL of PVA or Tween 80 solution (variable concentrations of 0.5, 1 and 2 % (Table I)). The resulting emulsion was continuously agitated in a glass reactor (600 mL, Ø = 80 mm) using a four-

TABLE I. Processing conditions for the formulations of microspheres

Code	PABA:EC ratio	Speed, rpm	Surfactant concentration, %	
			PVA	Tween 80
F11	1:1	600	1	—
F12	1:2	600	1	—
F13A	1:3	600	1	—
F14	1:4	600	1	—
F13B	1:3	600	0.5	—
F13C	1:3	600	2	—
F13D	1:3	900	1	—
F13E	1:3	1200	1	—
T13A	1:3	600	—	0.5
T13B	1:3	600	—	1

* 1 cP = 1 mPa s

-blade turbine impeller stirrer (blade length = 50 mm, blade width = 8 mm, IKA, RW20 digital, UK) at a constant stirring speed (speed variation 600, 900 and 1200 rpm) at room temperature for 4 h. The organic solvent was then allowed to evaporate in order to harden the oil droplets. The solidified microspheres were filtered, washed several times with deionized water and dried under vacuum in a desiccator containing CaCl_2 . The starting composition of the different microspheres prepared together with the formulation codes are summarized in Table I.

Microspheres characterization

Determination of the encapsulation efficiency. The PABA content in the microspheres was determined by dissolving 100 mg of dried microspheres in a sealed bottle containing 100 mL of absolute ethanol under stirring at a rotation speed of 250 rpm at 37 °C for 6 h. The resulting solution was analyzed for PABA content by UV–Vis spectroscopy. The actual drug loading (DL) and encapsulation efficiency (EE) of the microspheres were calculated using the following equations:

$$DL = 100(\text{Drug mass in microspheres}/\text{Mass of microspheres}) \quad (1)$$

$$EE = 100(\text{Actual drug loading}/\text{Theoretical drug loading}) \quad (2)$$

Particle size

The mean particle size and size distribution (δ) of microspheres were determined by scanning electron microscopy (SEM, Quanta 200 FEI) and optical microscopy (Optika 4083.B1). At least 500 microspheres were analyzed for each preparation and the mean diameter was calculated. The particle size distribution was calculated from various equations,^{22,23} the Sauter mean diameter, $d_{32} = \sum n_i d_i^3 / \sum n_i d_i^2$; the distribution δ , calculated as d_{43}/d_{10} ; the number mean diameter, $d_{10} = \sum n_i d_i / \sum n_i$; the weight mean diameter, $d_{43} = \sum n_i d_i^4 / \sum n_i d_i^3$, where i represent an index of the population and d_i is the particle diameter of the population i .

Scanning electron microscopy (SEM)

The morphology and surface topography of the prepared microspheres were examined without sputter deposition using a scanning electron microscope (SEM Quanta 200 FEI) at 50 Pas under 12 kV acceleration voltage. The microspheres were mounted on a double-scotched carbon film fixed on a stub.

Infrared spectroscopy

The samples were characterized by infrared spectroscopy using a Bruker Alpha FT-IR spectrometer, equipped with an Alpha platinum ATR with single reflection and diamond ATR module. The infrared spectra of pure PABA, blank ethylcellulose microspheres and the loaded microspheres were analyzed without any prior preparation.

Differential scanning calorimetry (DSC)

Thermal analysis (DSC) was performed on the microspheres using a Netzsch DSC 200 PC differential scanning calorimeter. All the samples were prepared by weighing (≈ 14 mg of pure PABA, ≈ 32 mg of blank ethylcellulose microspheres and the loaded microspheres) into hermetically sealed aluminum pans. The analysis was performed at a rate of 5 °C min⁻¹ within the temperature range 20–300 °C.

XRD analysis

The XRD patterns of pure PABA, blank ethylcellulose microspheres and the loaded microspheres formulations were recorded with a D8 Avance Bruker diffractometer in the 2θ range from 5 to 70°.

In vitro PABA H^+ release

The *in vitro* release studies of the PABA-loaded ethylcellulose microspheres were carried out using an appropriate glass dissolution reactor^{14,20} plunged in a bath regulated at 37 ± 0.5 °C. This reactor allows us to withdraw solution without microspheres. The PABA H^+ release kinetics from microspheres was followed by using UV-Vis spectrometer (Shimadzu UV-Vis 2401 PC, Japan) with a cell compartment thermostat at 37 °C. At the desired time, 100 mg of microspheres was soaked in 500 mL of buffer solution²¹ pH 1.2. The dispersion medium was stirred at a rotation speed of 250 rpm; at predetermined time intervals, 3 mL of solution was withdrawn, analyzed for PABA H^+ concentration by UV spectroscopy at 220 nm, and replaced in the reactor.

RESULTS AND DISCUSSION

Microspheres characterizations

The surface and morphology of the microspheres were studied using SEM (Figs. 1 and 2). The formulation parameters of the various prepared PABA-loaded ethylcellulose microspheres are summarized in Table I.

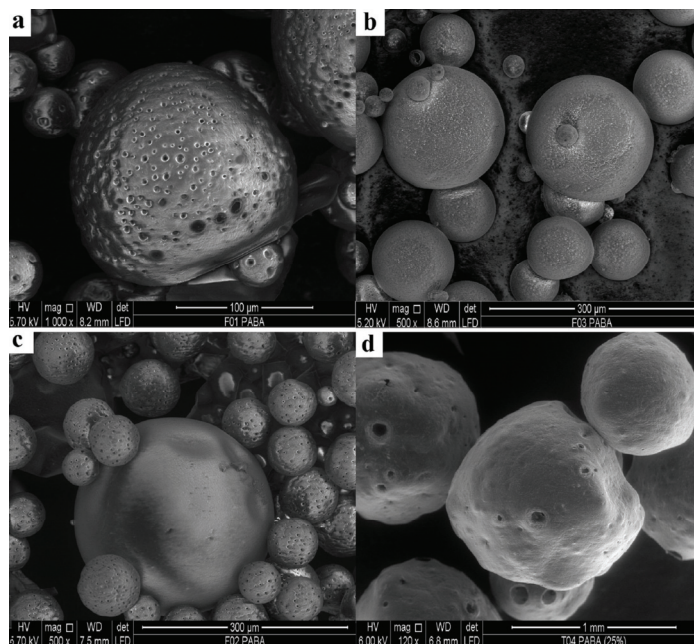


Fig. 1. SEM micrographs of the loaded microspheres. Preparation conditions: a) F13A, 1 % PVA, b) F13B, 0.5 % PVA, c) F13C, 2 % PVA and d) T13B, 1 % Tween 80. The microspheres were prepared with the PABA:EC ratio of 1:3 and stirring speed of 600 rpm.

The effect of the surfactants PVA and Tween 80 on the microspheres prepared under the same operative conditions (1:3 PABA:EC ratio and 600 rpm stirring speed) are shown in Fig. 1. The PVA microspheres (Fig. 1a) are spherical

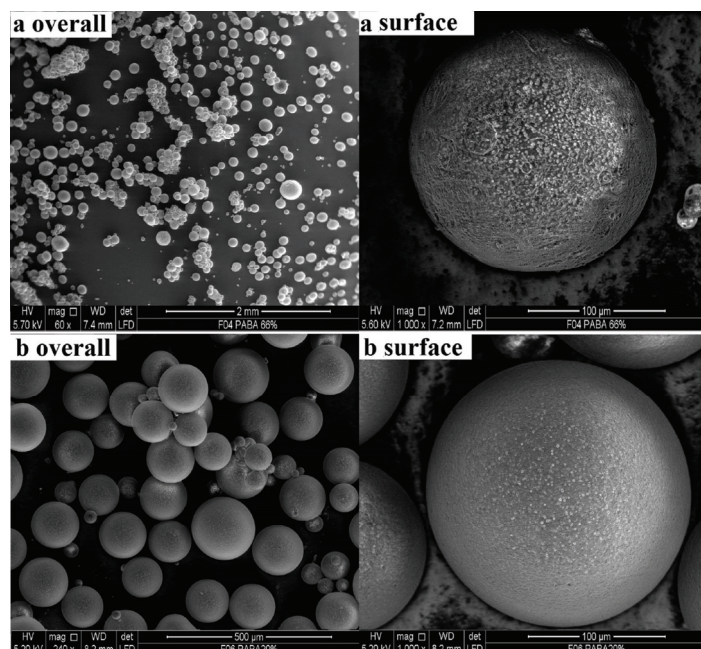


Fig. 2. SEM micrographs of the surface and morphology of the loaded microspheres prepared with different PABA:EC ratios. Preparation conditions: a) F12, 1:2 PABA:EC ratio and b) F14, 1:4 PABA:EC ratio. The microspheres were prepared with 1 % PVA at a stirring speed of 600 rpm.

and smaller than the Tween 80 microspheres with a rough and porous surface. It is obvious that the surface of these particles obtained with Tween 80 is much rougher with bigger pores in the surface (Fig. 1d). Indeed, we have obtained microspheres with a mean Sauter diameter (d_{32}) in the range 121 to 143 μm with PVA and in the range 793 to 870 μm with Tween 80 (Table II). Comparative effects between PVA and Tween 80 described in Table II show their direct action on the actual drug loading (DL), encapsulation efficiency (EE), the mean Sauter diameter (d_{32}) and the distribution (δ) of these microparticulate systems. Small microsphere sizes were obtained with PVA. This observation is in agreement with the literature.¹⁵ Furthermore, PVA acts more strongly than Tween 80 on the reduction of the interfacial tension decreasing the coalescence of the emulsion droplets. Increasing the PVA concentration promotes both the actual drug loading and encapsulation efficiency, decreases the mean diameter d_{32} and the distribution (δ). In the present research, PVA gave a higher EE than Tween 80. This could be explained by the structure, the ratio 1:3 of PABA:EC, stirring speed at 600 rpm and the porosity in the surface of these microparticles. For Tween 80, the presence of large pores in the surface of the particles led to an important loss of PABA, resulting in a decrease of DL and EE . A comparison of the SEM

images in Fig. 1a and d (F13A and T13B) performed at the same surfactant concentration (1 %) PVA and Tween 80, respectively, reinforce these conclusions.

TABLE II. The effects of various processing conditions on the characteristics and encapsulation results for the prepared microspheres; *DL* – drug loading and *EE* – encapsulation efficiency

Code	<i>DL</i> / %		<i>EE</i> / %	<i>d</i> ₁₀ / μm	<i>d</i> ₃₂ / μm	<i>d</i> ₄₃ / μm	<i>δ</i>
	Theoretical	Actual					
F11	50.00	25.10	50.20	80.95±2.00	90.00±0.67	148.45±2.61	1.83±0.01
F12	33.33	19.45	58.35	73.15±0.52	106.04±0.50	127.73±0.61	1.74±0.02
F13A	25.00	16.85	67.40	87.45±1.98	121.11±2.97	147.21±0.50	1.69±0.04
F14	20.00	15.81	79.05	114.73±1.12	164.61±0.72	182.17±0.79	1.59±0.01
F13B	25.00	15.26	61.04	83.83±1.64	142.91±3.34	159.54±3.84	1.90±0.08
F13C	25.00	17.55	70.20	69.02±2.79	77.54±1.26	91.13±2.93	1.31±0.01
F13D	25.00	14.06	56.24	64.05±0.78	62.74±0.08	94.46±0.84	1.47±0.00
F13E	25.00	13.00	52.00	40.05±0.09	47.04±0.11	50.12±0.68	1.25±0.02
T13A	25.00	09.38	37.52	441.30±0.69	869.28±1.06	987.45±3.87	2.23±0.01
T13B	25.00	12.52	50.08	397.64±3.36	793.21±2.55	965.58±0.99	2.42±0.02

The spherical microspheres prepared under the same operative conditions with different PABA:EC ratios, 1:2 and 1:4, are shown in Fig. 2. The microspheres formulated at the higher EC content 1:4 (F14) showed a smooth and homogenous surface without any visible pores (Fig. 2b). Some microspheres had a rough and porous surface when a 1:2 PABA:EC ratio was used (Fig. 2a). An increase in the microspheres sizes (*d*₃₂) was observed with increasing amount of EC (Table II). It was reported that increasing the viscosity of the organic phase by increasing the polymer concentration yields larger microspheres.^{24,25} On increasing the amount of EC from 1:1 to 1:4, the encapsulation efficiency increased from 50.20 to 79.05 % with 1 % PVA at a constant stirring speed of 600 rpm. This could be explained by the fact that increasing the viscosity of the dispersed droplets hindered the loss of PABA.^{19,26}

The mean particle size and size distribution could be determined by the operative conditions of the microencapsulation process.^{25–28} From the results of microspheres sizes (Table II), it was observed that under the same operative conditions, increasing stirring speed from 600 to 900 rpm and to 1200 rpm affected the microspheres characteristics: the mean Sauter diameter (*d*₃₂) was decreased from 121.11 to 62.74 μm and to 47.04 μm, the distribution (*δ*) was improved from 1.69 to 1.47 and to 1.25 and the encapsulation efficiency (*EE*) decreased from 67.4 to 52.0 %. The obtained results concerning the particle size was also reported by André-Abrant *et al.*²⁵

The infrared spectra of the microspheres are compared with the PABA and the polymer matrix EC spectra in Fig. 3. The analysis showed the presence of similar characteristic bands of the microspheres in the PABA-loaded microspheres

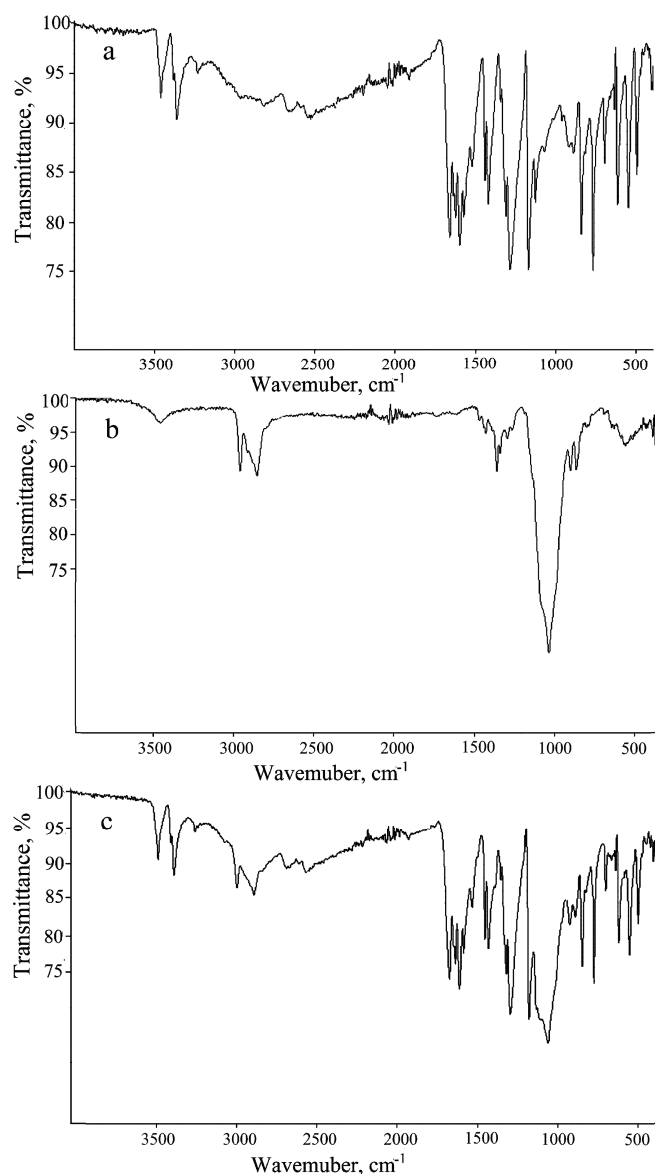


Fig. 3. Infrared spectra of: a) pure PABA, b) blank ethylcellulose microspheres and c) the loaded microspheres F14.

F14 at the same wavenumbers: ($\nu(\text{C}-\text{OH})$) at 1659.60 and at 1285 cm^{-1} , the characteristic bands of COOH group,²⁹ ($\text{C}-\text{N}$) at 1343 cm^{-1} , the aromatic vibration band ($\text{C}=\text{C}$) at 1622 cm^{-1} and the amino group band ($\text{N}-\text{H}$) at 3359–3457 cm^{-1} . The spectrum of the PABA-loaded microspheres appeared as the sum of the spectra of pure PABA and EC.

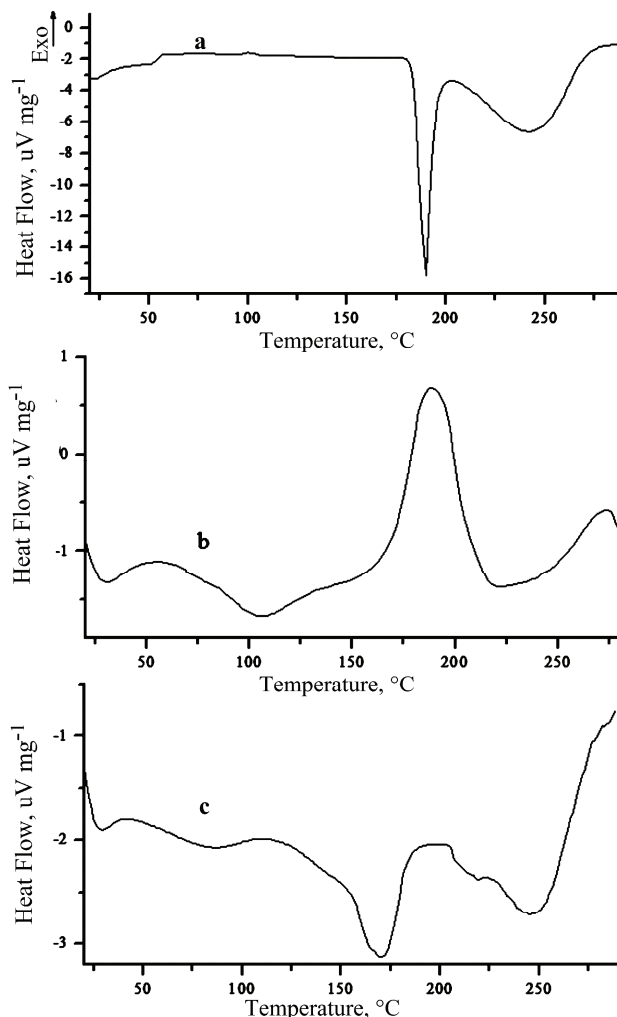


Fig. 4. DSC thermograms of: a) pure PABA, b) blank ethylcellulose microspheres and c) the loaded microspheres F14.

The compatibility of PABA in the microspheres formulations was studied by DSC (Fig. 4). On comparing the DSC curves in Fig. 4a–c, a sharp endothermic peak at 191 °C (lit. 190 °C), corresponding to the melting point of PABA, accompanied by an endothermic peak positioned at 250 °C were registered in Fig 4a. The loaded microspheres (Fig. 4c) showed a broad endothermic peak at 170 °C, indicating the melting point of PABA in the presence of EC. This change in the peak position could be a consequence of some interaction between polymer matrix EC and the drug. The thermal transition of the polymer in the ethylcellulose microspheres (blank test) was observed at \approx 85 °C, which corresponds to the glass

transition temperature (T_g) of EC. The T_g was difficult to detect, it generally depends on the molecular weight and the degree of substitution of the used EC. It was registered by other authors^{30–32} that the variability of the thermal transition temperature T_g depends on the structure of the EC and the addition of certain compounds, such as plasticizer, introduced to increase the porosity of the microspheres.³² The elongation, flexibility and T_g decreased significantly with increasing number of ethoxy groups in the EC.³⁰ At higher temperatures, two peaks one endothermic and the other exothermic appeared at 106–190 °C in the present case, Fig. 4b, which are usually observed for pure EC. The exothermic peak at around 190 °C is associated with oxidative degradation of the ethylcellulose.³⁰ Finally, the endothermic peak positioned at 250 °C in Fig. 4a and c accompany PABA and appears to be a compound derived from the possible degradation of PABA at temperatures higher than its melting point at 191 °C. In conclusion, the microspheres were well loaded with PABA, a fact also attested by its release in the simulated solution of pH 1.2.

The XRD technique was used together with DSC to study the physical state of the drug in the microspheres. The crystalline nature of PABA was clearly demonstrated by its characteristic XRD pattern containing well-defined peaks within the 2θ range from 5 to 70° (Fig. 5). However, the PABA-loaded ethylcellulose microspheres exhibited a characteristic diffraction pattern that was less intense as compared to that of pure PABA.

Kinetics of in vitro PABA H^+ release

To analyze the drug release kinetics, the cumulative release data *versus* time were fitted to the Higuchi³³ and the Korsmeyer–Peppas equations.^{34,35} The Higuchi model describes drug release by a simple equation of the type:

$$Q_t = k_H t^{1/2} \quad (3)$$

where Q_t is the cumulative percent of drug released at time t and k_H is a constant characteristic of the process. The cumulative PABA H^+ release was proportional to square root of time suggesting that the drug release from microspheres was diffusion controlled (Fig. 6). The calculated values of the rate constants k_H were influenced by the process parameters: stirring speed, surfactant nature and concentration, and the amount of polymer matrix EC. The best fit with the highest correlation coefficient r^2 was observed in the Higuchi model (Table III). The obtained values of rate constants (k_H) decreased with increasing amount of polymer, decreasing surfactant concentration and stirring speed. Furthermore, to determine the mechanism of drug release, the obtained release *versus* time data were fitted to the Korsmeyer and Peppas semi-empirical equation as follows:

$$\frac{M_t}{M_{t\infty}} = k_{KP} t^n M_t \quad (4)$$

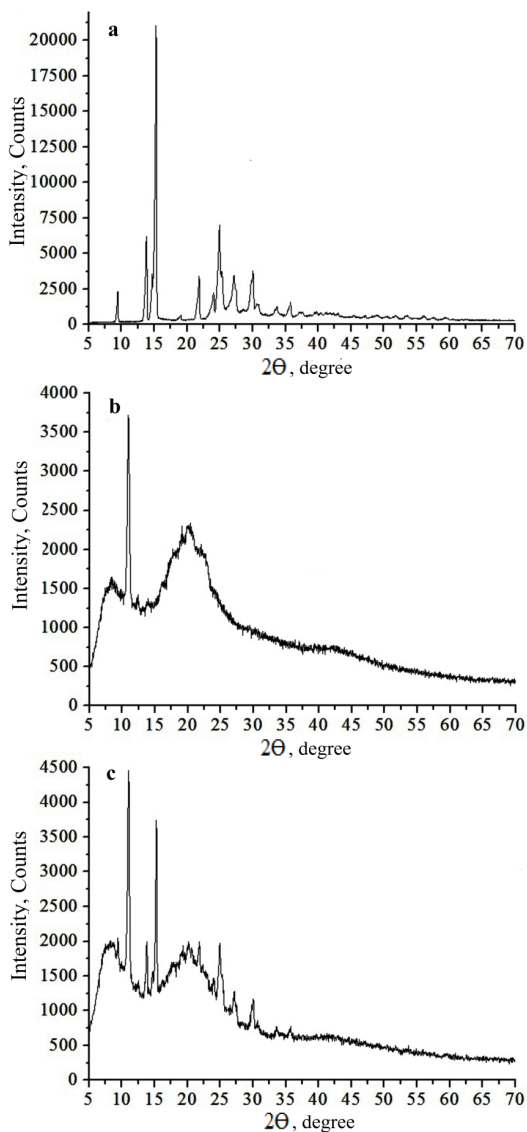


Fig. 5. XRD patterns of a) pure PABA, b) blank ethylcellulose microspheres and
c) loaded microspheres F14.

where $M_t/M_{t\infty}$ is the fraction of drug released at time t , M_t and $M_{t\infty}$ represent the masses of drug released at time t and t_∞ , respectively, k_{KP} is the rate constant and n is an empirical parameter characterizing the release mechanism. The values of n , k_H (Higuchi) and k_{KP} (Korsmeyer–Peppas) were estimated for all formulations by application of these equations and the obtained values are given in Table III. Divers' values of n for cylinders and spheres were described by Ritger and

Peppas.^{34,36} For spherical geometry, a value of $n = 0.43$ corresponds to Fickian diffusion (Case I), $n = 0.85$ to Case II transport (zero order release) and $n > 0.89$ to Super Case II drug release. Intermediary values ranging between 0.43 and 0.85 are attributed to anomalous or non-Fickian transport (erosion and diffusion).³⁶ The values of n for the microspheres prepared by varying the process parameters range from 0.29 to 0.39 (Table III), indicating a shift of Fickian transport. For the Korsmeyer–Peppas model, the values of the rate constants depended on the obtained n values.

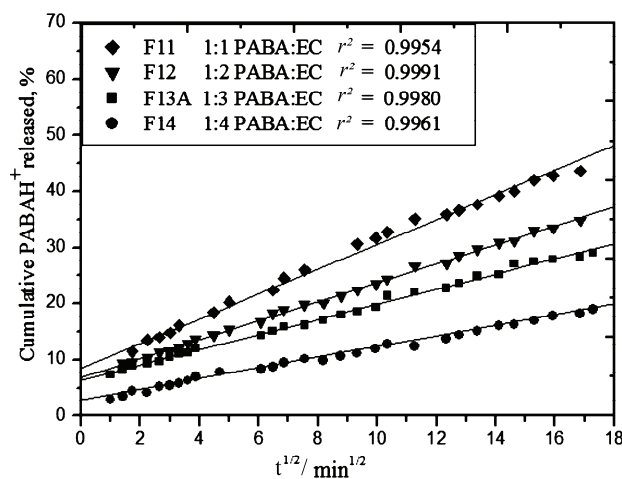


Fig. 6. Higuchi plots of % PABAH^+ released from microspheres in pH 1.2 buffer at 37 °C for different PABA:EC ratios with the PVA concentration constant at 1 % and the stirring speed constant at 600 rpm.

TABLE III. Release kinetic parameters of the model equations applied to the *in vitro* release of PABAH^+ from microspheres; k_{H} and k_{KP} – the release rate constants for the Higuchi and Korsmeyer–Peppas model, respectively; n – the release exponent of the Korsmeyer–Peppas model; r^2 – the correlation coefficient

Code	Kinetic model				
	Higuchi		Korsmeyer–Peppas		
	$k_{\text{H}} / \text{min}^{-1/2}$	r^2	n	$k_{\text{KP}} / \text{min}^{-n}$	r^2
F11	2.209	0.9954	0.29	0.00066	0.9971
F12	1.689	0.9991	0.31	0.00039	0.9971
F13A	1.349	0.9980	0.30	0.00029	0.9932
F14	0.936	0.9967	0.39	0.00033	0.9881
F13B	1.182	0.9950	0.37	0.00040	0.9937
F13C	2.061	0.9970	0.34	0.00055	0.9963
F13D	2.155	0.9982	0.33	0.00051	0.9952
F13E	2.468	0.9969	0.32	0.00075	0.9962
T13A	1.415	0.9956	0.29	0.00032	0.9955

The influence of different process parameters and the content of matrix polymer on the release rate of the active agent were studied. The plots of cumulative PABAH^+ released versus time from different microspheres formulations are shown in Figs. 7 and 8. After the end of 24 h of dissolution, the percentages of PABAH^+ released from microspheres F11, F12, F13A and F14 were 67.62, 56.65, 51.53 and 43.47 %, respectively (Fig. 7). This study indicated that the release rate decreased with higher polymer (EC) concentrations. Increasing the amount of polymer from 1:1 to 1:4 decreased the PABAH^+ release rate due to the lower porosity of the surface of the microspheres (Fig. 2a and b). On increasing the amount of EC, the drug loading (*DL*) increased.

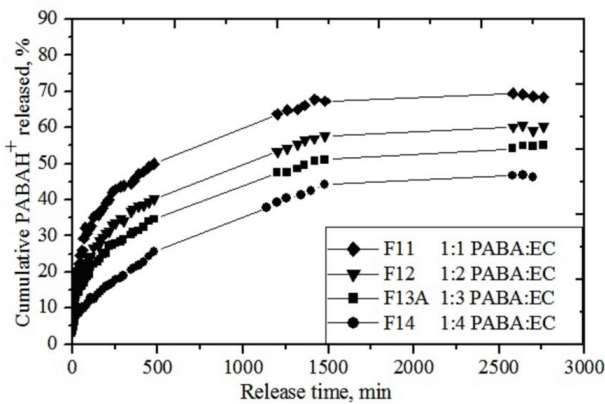


Fig. 7. Cumulative release of PABAH^+ from the microspheres in pH 1.2 buffer at 37 °C with different PABA:EC ratios with the PVA concentration constant at 1 % and the stirring speed constant at 600 rpm.

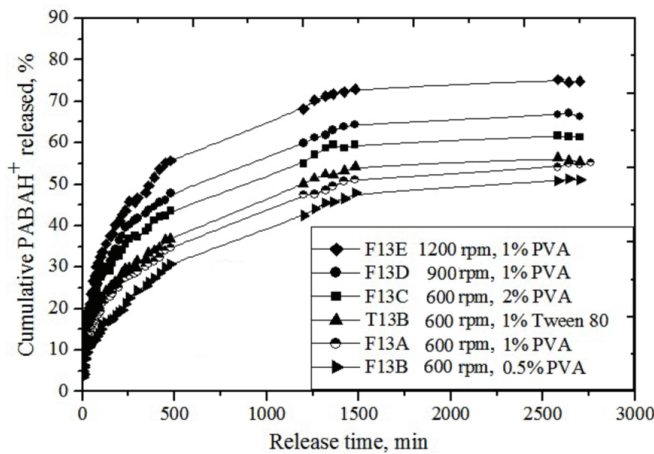


Fig. 8. Cumulative release of PABAH^+ % from the different microspheres in pH 1.2 buffer at 37 °C (with the PABA:EC ratio constant at 1:3).

Nevertheless, the release rate was faster. However, a significant effect of the stirring speed on the size and distribution (δ) of the microspheres was registered. Increasing stirring speed by decreasing the size (d_{32}) and the size distribution ($\delta = 1.25$) of the microspheres led to a faster release rate (Fig. 8). The release of the active agent was inversely proportional to the size of the microspheres.^{37,38} Figure 8 shows that the cumulative release was more rapid from the smaller microspheres prepared at a high PVA concentration. It was reported that for the smaller microspheres, the larger effective area produces a greater number of drug molecules at the surface of the microspheres, which leads to a faster drug release.²⁰ The release rate from microspheres T13B prepared with Tween 80 in the aqueous phase was more rapid than that observed with PVA, this is due to the porosity and the surface morphology of these microspheres (Fig. 1d). Thus, the results showed that the PABAH^+ release rate from these systems could be modulated by adjusting the formulation processing parameters.

CONCLUSIONS

The present study demonstrated the effects of formulation process parameters on the characteristics and *in vitro* release behavior of PABA-loaded ethylcellulose microspheres prepared by microencapsulation using the solvent evaporation technique. It was shown that the surfactant nature could minimize the loss of PABA, affect size and structure morphology of the microspheres. PVA gives perfectly spherical microspheres with a smooth and porous surface while Tween 80 led to slightly spherical shapes with a rough surface and large pores. Systems with large size ranges (the mean Sauter diameter d_{32} in the range 47 to 165 μm with PVA and 793 to 870 μm with Tween 80) were obtained by modifying the process conditions. The particle size (d_{32}) and distribution (δ) can be successfully controlled by the choice of the nature and concentration of the surfactant, stirring speed, and the amount of polymer. The encapsulation efficiency (EE) can be improved especially by increasing the PVA concentration and the amount of EC. The release kinetics using Higuchi and Korsmeyer–Peppas equations showed a Fickian diffusion mechanism and the release rate could be controlled by adjusting the microencapsulation processing parameters that have significant effects on the particle size.

ИЗВОД

УТИЦАЈ ПРОЦЕСНИХ ПАРАМЕТара НА ЕФИКАСНОСТ ИНКАПСУЛАЦИЈЕ И
КОНТРОЛИСАНО ОТПУШТАЊЕ *p*-АМИНОБЕНЗОЕВЕ КИСЕЛИНЕ ИЗ МИКРОСФЕРА
НА БАЗИ ЕТИЛ-ЦЕЛУЛОЗЕ

MERYEM MOUFFOK¹, ABDERREZZAK MESLI¹, ILHAM ABDELMALEK¹ и ETIENNE GONTIER²

¹Laboratory of Physical and Macromolecular Organic Chemistry, Faculty of Exact Sciences, University of Djillali Liabes, Sidi Bel-Abbes, Algeria и ²Bordeaux Imaging Center–UMS 3420, Victor Segalen, University of Bordeaux, France

У овом истраживању, *p*-аминобензоева киселина је инкапсулирана у микросфере на бази етил-целулозе емулзионим поступком (уље/вода) отпаравањем лако испарљивог растварача. Варијани су следећи процесни параметри: масени однос *p*-аминобензоева киселина/етил-целулоза (PABA/EC), брзина мешања, врста емулгатора и њихова концентрација како би се изучавао њихов утицај на ефикасност инкапсулатије и брзину отпуштања лека из полимерне матрице. SEM анализа је показала да су добијене сферне микрочестице, порозне структуре и различите морфологије. У присуству PVA су формиране микрочестице са средњим Саутеровим пречником (d_{32}) у опсегу од 47 до 165 μm, а у присуству Tween 80 у опсегу од 793 до 870 μm уз подешавање осталих процесних параметара. Ефикасност инкапсулатије је била у опсегу од 37,52 до 79,05 % и показала се погодном за продужено отпуштање *p*-аминобензоеве киселине. Микросфере су карактерисане помоћу FTIR, DSC и XRD. Отпуштање катјона *p*-аминобензоеве киселине је пратено на pH 1,2 и 37±0,5 °C у медијуму који симулира услове у желуцу, помоћу UV–Vis анализе. Добијени профили при праћењу отпуштања лека су најбоље одговарали Higuchi моделу, са високим степеном корелације (r^2), а добијене вредности n из Korsmeyer–Peppas једначине су показале да отпуштање лека одговара механизму Фикове дифузије.

(Примљено 8. марта, ревидирано 28. јуна, прихваћено 1. јула 2016)

REFERENCES

1. W. B. Pratt, *Fundamentals of Chemotherapy*, Oxford University Press, London, 1973
2. M. Elson, *Staying healthy with nutrition, the complete guide to diet and nutritional medicine*, Celestial Arts Publishers, Berkley, CA, 2006
3. S. I. Akberova, P. I. Musaev Galbinur, *Vestn. Oftalmol.* **116** (2000) 16
4. S. I. Akberova, E. Tazulakhova, V. Mamedova, *Vestn. Oftalmol.* **122** (2006) 23.
5. M. E. Crisan, P. Bourosh, M. Maffei, A. Forni, S. Pieraccini, M. Sironi, *PlosOne* **9** (2014) 1
6. S. I. Akberova, *Biol. Bull.* **29** (2002) 390
7. P. Lahmani, L. Simoneau (Roussel Uclaf), EP 0509904-B1, 1996
8. S. M. MacDonald, M. Caunt, P. C. Brooks, S. C. Farmenti, *Int. J. Radiat. Oncol. Biol. Phys.* **60** (2004) 352
9. R. S. Sharma, R. C. Joy, C. J. Boushey, M. G. Ferruzzi, A. P. Leonov, M. A. McCrory, *J. Acad. Nutr. Diet.* **114** (2013) 457
10. M. Mirzaei, M. Khayat, A. Saeidi, *Sci. Iran.* **19** (2012) 561
11. A. Albert, E. Sergeant, *The Determination of Ionization Constants*, Chapman and Hall, London, 1971
12. V. Ramesh Babu, K. S. V. Krishna Rao, Y. Lee, *Polym. Bull.* **65** (2010) 157
13. Y. Y. Yang, T.-S. Chung, N.-P. Ng, *Biomaterials* **22** (2001) 231
14. Z. El Bahri, J.-L. Taverdet, *Powder Technol.* **172** (2007) 30
15. M. Li, O. Rouaud, D. Poncelet, *Int. J. Pharm.* **363** (2008) 2616
16. R. K. Deshmukh, J. B. Naik, *Mater. Sci. Eng., C* **48** (2015) 197

17. R. Dinarvand, N. Sepehri, S. Manoochehri, H. Rouhani, F. Atyabi, *Int. J. Nanomed.* **6** (2011) 877
18. K. Diaf, Z. El Bahri, N. Chafi, L. Belarbi, A. Mesli, *Chem. Pap.* **66** (2012) 779
19. N. T. Hwisa, P. Katakam, B. Chandu, S. K. Adiki, *VRI Biol. Med. Chem.* **1** (2013) 8
20. I. Abdelmalek, I. Svahn, S. Mesli, G. Simonneaux, A. Mesli, *J. Mater. Environ. Sci.* **5** (2014) 1799
21. United States Pharmacopeia (USP 27), *The National Formulary (NF 22)*, 2004
22. K. KaczmarSKI, J. C. Bellot, *Acta Chromatogr.* **13** (2003) 22
23. C. Jégat, J. L. Taverdet, *Polym. Bull.* **44** (2000) 345.
24. C. Y. Yang, S. Y. Tsay, R. C. Tsiang, *J. Microencapsulation* **17** (2000) 269
25. A. André-Abrant, J. L. Taverdet, J. Jay, *Eur. Polym. J.* **37** (2001) 955
26. R. C. Mehta, B. C. Thanoo, P. P. DeLuca, *J. Controlled Release* **41** (1996) 249
27. E. Schlicher, N. S. Postma, J. Zuidema, H. Talsma, W. Hennink, *Int. J. Pharm.* **153** (1997) 235
28. H. Jeffery, S. Davis, D. T. O'Hagan, *Pharm. Res.* **10** (1993) 362
29. R. M. Silverstein, G. C. Bassler, T. C. Morill, *Spectrometric Identification of Organic Compounds*, 4th ed., Wiley, New York, 1981
30. H. L. Lai, K. Pitt, D. Q. M. Craig, *Int. J. Pharm.* **386** (2010) 178
31. C. T. Şengel-Turk, C. Hasçiçek, N. Gönül, *AAPS PharmSciTech* **12** (2011) 1127
32. M. K. Das, K. Rama Rao, *Acta Pol. Pharm.* **63** (2006) 141
33. S. Dash, P. N. Murthy, L. Nath, P. Chowdhury, *Acta Pol. Pharm.* **67** (2010) 217
34. P. L. Ritger, N. A. Peppas, *J. Controlled Release* **5** (1987) 23
35. J. Crank, *The mathematics of diffusion*, 2nd ed., Clarendon, Oxford, 1976, p. 85
36. R. W. Korsmeyer, E. Von Merwall, N. A. Peppas, *J. Polym. Sci.*, **24** (1986) 409
37. F. Gabor, B. Ertl, M. Wirth, R. Mallinger, *J. Microencapsulation* **16** (1999) 1
38. Z. Urbán-Morlán, S. E. Mendoza-Elvira, R. S. Hernández-Cerón, S. Alcalá-Alcalá, H. Ramírez-Mendoza, A. Ciprián-Carrasco, E. Piñón-Segundo, D. Quintanar-Guerrero, *J. Mex. Chem. Soc.* **59** (2015) 173.